Embedding of Gold Nanoclusters on Polystyrene Surfaces: Influence of the Surface Modification on the Glass Transition

R. Weber,*,† I. Grotkopp,† J. Stettner,† M. Tolan,‡ and W. Press†,§

Institut für Experimentelle und Angewandte Physik, Christian-Albrechts-Universität, Leibnizstrasse 17-19, 24098 Kiel, Germany, and Experimentelle Physik I, Universität Dortmund, 44221 Dortmund, Germany

Received June 27, 2003; Revised Manuscript Received September 8, 2003

ABSTRACT: The thermal behavior of surfaces of polystyrene (PS) films of 80−100 nm thickness decorated with gold nanoclusters with radii ranging from 9 to 18 Å has been investigated by in situ X-ray reflectivity measurements. Recently, the embedding of tiny clusters—driven by the large difference between the surface energies of the metal and the polymer—has been proposed to serve as a nanoprobe of the glass transition temperature T_g^s at the polymer surface. In the present work for the first time a systematic study of the embedding process with a variable amount of metal has been carried out. Determining the density profile by X-ray reflectivity measurements, we monitored simultaneously the onset of the embedding at a temperature T_e and the glass transition temperature T_g^f of the whole film, which corresponds to the bulk value T_g^b. We show that at sufficiently low coverages the gold clusters begin to embed at temperatures T_e well below T_g^f, which reveals the presence of a surface layer with an increased mobility of the polymer chains. Furthermore, it turned out that there is a strong effect due to the attractive polymer−metal interactions which again suppresses the kinetics at the surface and thus leads to an increase of T_e with higher gold coverages. Therefore, the embedding temperature T_e can be regarded as an upper limit for the glass transition temperature T_g^s of the free polymer surface. In the present study we found for polystyrene with molecular weight $M_w = 220$ kg/mol ($M_w = 3.7$ kg/mol) a reduction for the surface glass transition of more than 37 K (22 K) with respect to its bulk value.

1. Introduction

The mechanical, rheological, and thermal behavior of polymer surfaces is an important field of research. This is not only related with technical applications,[1] e.g., in the field of microelectronics,[2] but also with a general physical interest in polymers under confinement and at surfaces and interfaces. In such cases the behavior of the polymer is in general substantially different from that in the bulk.

Starting 10 years ago the work concentrated on the thermal behavior of thin films. It was found experimentally that the glass transition temperature of the film, T_g^f, usually was changed when the polymer film thickness was below a certain limit,[3−7] e.g., below about 60 nm for high molecular weight polystyrene. Both an increase or a decrease in T_g^f were observed, depending on the polymer−substrate interaction.[5,8] A comprehensive summary is given in ref 9. Theoretical calculations about the change of the glass transition in thin polymer films, which also take into account the film−substrate interactions, have confirmed the experimental results.[10,11]

The aforementioned works explained the thin-film behavior by the ratio of mobile polymer chain segments near the surface to those in the less mobile bulk, which increases with decreasing film thickness. To obtain information that solely originates from the polymer surface, several experimental methods have been used. They focused in particular on the examination of the glass transition or related properties of the polymer surface, e.g., the viscoelastic response due to mechanical stimulation.

Mainly three classes of experiments have been carried out: (1) A large number of investigations were done by the use of scanning probe microscopy methods. Either frictional forces or adhesion or shear forces were used to gain information on the viscoelastic properties of the surface. Depending on the method applied, different results were obtained.[12−18] Either changes near T_g^b or well below T_g^b are reported. Whether these methods really probe the surface or actually monitor bulk properties is still controversially discussed.[19]

(2) Another class of experiments concentrated on the observation of changes of the surface morphology upon heating above the glass transition temperature.[20−22] In ref 20, for example, changes in artificially roughened polymer surfaces are reported for temperatures below T_g.

(3) The third class is based on the embedding of small particles that occurs due to the differences in cohesive energy between the polymer and the clusters. Studies by X-ray photoemission spectroscopy (XPS) have been performed recently.[23,24] In these works the penetration depth of the photoelectrons emerging from the metal plays the major role in the detection of the embedding process. With increasing temperature the emerging polymer layer on top of the particles causes a reduction of the detected photoelectrons of the metal due to absorption. Further studies on the embedding of nanosize clusters were performed by the application of atomic force microscopy (AFM).[25,26]

An alternative method provides the determination of the electron density profile by X-ray reflectometry. The profile can be determined with a high vertical accuracy, which is necessary in order to monitor the growth of a

† Christian-Albrechts-Universität.
‡ Universität Dortmund.
§ Present address: Institut Laue-Langevin, 38042 Grenoble, France.

10.1021/ma034880o CCC: $25.00 © 2003 American Chemical Society
Published on Web 10/30/2003

polymer layer above the clusters accompanied by the embedding process.

Measurements on polystyrene−gold samples have been performed before with relatively large nominal gold layer thicknesses $d_n = 10$ Å and $d_n = 20$ Å.[27] This work concentrated on the broadening of the cluster layer perpendicular to the surface due to diffusion by Brownian motion above the glass transition temperature. Because of the large values of d_n, the growth of the polymer layer on top of the clusters was hardly visible. By the preparation of *low* amounts of gold, as it is done in the present work, not only this problem has been overcome, but also the analysis and interpretation of the data are significantly facilitated. Since the clusters are almost spherical,[28,29] the description of the interfaces in the electron density profile can be done by a simpler model than those needed in ref 27. Besides, the changes in the electron density profile due to the embedding process are not dominated by the huge amount of gold. Details are given in sections 2 and 3.

From the aforementioned studies the question arises, to what extent does the change of the polymer surface due to the presence of the clusters influence the glass transition at the surface and hence the measured quantities?

The aim of the present work is to determine the embedding temperature T_e, describing the onset of the embedding process, as a function of the cluster size and the number density of the clusters. The influence of the polymer−cluster interaction and the role of the cluster size will be discussed.

2. Experimental Section

2.1. Materials and Sample Preparation. Polystyrenes of two different molecular weights of $M_w = 3.7$ kg/mol ($M_w/M_n = 1.08$) and $M_w = 220$ kg/mol ($M_w/M_n = 1.05$) were used in this study. The polymers were purchased from Aldrich and Fluka.

Polystyrene films were spin-coated from toluene solution onto silicon wafers from Wacker Siltronic without a removal of the native oxide layer. The thickness of the polymer layer was chosen to $d_{PS} = 80-100$ nm. This thickness ensures that the Si/SiO_x substrate does not influence the polymer at the surface, since it clearly exceeds characteristic length scales of the polymer such as the mean end-to-end distance R_0 or twice the radius of gyration R_g. For the highest molecular weight samples of $M_w = 220$k these lengths are $R_0 = 32$ nm and $R_g = 13$ nm.

The polystyrene films have been annealed for 12 h in high vacuum of pressure $p < 1 \times 10^{-6}$mbar at appoximately 30 K above the bulk glass transition temperature T_g^b followed by slow cooling to room temperature at a rate of 0.33 K/min to remove the remaining solvent and to relax the samples as much as possible.

Subsequently, the samples were transferred into a vacuum chamber with a base pressure of $p \approx 10^{-9}$ mbar. The preparation of the nanoclusters was performed by thermal evaporation of gold purchased from Goodfellow with a purity of more than 99.99%. The gold was evaporated from a Molybdenum crucible onto the polymer surface−held at room temperature (about 300 K)−with the low rate of $r_p = 0.5$ Å/min. The total pressure in the chamber during the preparation was $p \approx 2 \times 10^{-8}$ mbar. The evaporation rate r_p and the nominal gold layer thickness $d_n = r_p t_p$ with the preparation time t_p were controlled by a quartz crystal monitor.

The surface tension of the polymer and the metal differ by almost 2 orders of magnitude. Therefore, at the low evaporation rate chosen and for nominal gold layer thicknesses $d_n <$ 10 Å spherical clusters form, which are almost monodispersive. The mean cluster radii of the samples prepared for this study vary between $r_c = 9$ Å for $d_n = 0.3$ Å and $r_c = 18$ Å for $d_n = 9$ Å. The corresponding fractions f of the surface covered by clusters vary from 2% to about 37%, and the number densities from $n_c = f/(\pi r_c^2) \approx 1 \times 10^{12}$ cm^{-2} to $n_c \approx 3.5 \times 10^{12}$ cm^{-2} (see Table 1).

Table 1. Overview of the Investigated Samples[a]

M_w [kg/mol]	d_n [Å]	r_c [Å]	f	n_c [10^{12} cm^{-2}]	T_e [K]	T_g^f [K]
3.7	0.3	9	0.02	0.8	321.0 ± 3.2	343.4 ± 3.0
	0.7	12	0.05	1.1	330.6 ± 4.0	350.9 ± 2.0
	0.9	12	0.06	1.3	333.9 ± 2.5	343.3 ± 2.5
	3.9	14	0.22	3.6	345.0 ± 3.0	343.1 ± 3.5
	7.6	17	0.35	3.9	355.5 ± 2.5	348.1 ± 3.0
220	0.8	11	0.05	1.3	334.3 ± 3.0	371.2 ± 2.0
	1.5	10	0.11	3.5	343.7 ± 3.5	369.6 ± 2.0
	2.8	14	0.14	2.8	359.3 ± 3.0	372.2 ± 2.5
	9.1	18	0.37	3.6	368.7 ± 3.5	369.6 ± 3.0
220	16.7	(25)	0.50	2.5	no embedding	372.3 ± 2.5

[a] The first two columns show the preparation parameters with M_w, the weight-average molecular weight of the polystyrene films, and d_n, the nominal gold layer thickness. The next three columns state the parameters extracted from the electron density profiles at room temperature with r_c, the mean cluster radius, f, the fraction of the surface covered by gold clusters, and n_c, the number density of the clusters. In the last two colums the determined embedding temperatures T_e and the glass transition temperatures T_g^f of the films are listed. The sample with $M_w = 220$k and $d_n = 16.7$ Å serves as an example with no embedding observed. It is not further used in the analysis.

It is noteworthy that at small nominal thicknesses $d_n < 1.5$ Å the number density of the clusters steeply increases from $n_c \approx 1 \times 10^{12}$ cm^{-2} to $n_c \approx 3.5 \times 10^{12}$ cm^{-2} with increasing values of d_n, while for 1.5 Å $< d_n <$ 9 Å it remains almost constant at $n_c \approx 3.5 \times 10^{12}$ cm^{-2}. In the context of nucleation and growth theory the former period is referred to as the nucleation phase, and the latter is called the growth phase.[30]

The values for r_c, f, and n_c have been extracted from the density profiles gained from the reflectivity data assuming monodispersive clusters with a depth variation similar to the roughness $\sigma_{PS} = 4-5$ Å of the pure polymer surface. They are in excellent agreement with the values extracted from TEM micrographs of comparable samples.[28] These TEM images have also shown that the size distribution is only about 10% for nominal gold layer thicknesses of $d_n \approx 1$ Å and rises to about 30% for $d_n \approx 8$ Å. A model that explains the density profiles and additionally takes into account such a size variation is also possible, but not necessary, since it only slightly affects the determined radii and number densities.[29] Examples of how the cluster arrangement on a polymer surface might look like are given by the TEM micrographs in refs 31−33.

2.2. X-ray Reflectivity Measurements. In situ X-ray reflectivity measurements have been performed at the Hamburger Synchrotronstrahlungslabor HASYLAB at DESY at the beamline W1.1. The samples were mounted on a heatable copper plate in a vacuum cell ($p < 6$) $\times 10^{-6}$ mbar) in order to provide good temperature stability and to prevent dewetting of the PS films[34] at temperatures above T_g^f. The X-ray energy was $E = 10.5$ keV ($\lambda = 1.181$ Å). This is well below the L-edges of gold and was chosen to avoid fluorescence of the clusters but is sufficiently high to minimize radiation damages.

Figure 1 shows a sketch of the X-ray reflectivity experiment, which requires the angle α_i of the incident beam being equal to that of the final, reflected beam, α_f. Variation of $\alpha_i = \alpha_f$ provides a possibility of measuring the intensity of the vertical wave vector transfer $q_z = 2k \sin \alpha_i$, with $k = 2\pi/\lambda$.

Apart from the reason mentioned in section 2.1, the polymer layer thickness of $d_{PS} = 80-100$ nm is also a good choice with regard to the information that can be extracted from X-ray reflectivity measurements. At this thickness all interfaces contribute to the interference pattern observed in the scattered intensity, the so-called Kiessig fringes.[35] This condition is not fulfilled for much thicker samples for which the resolution limit of the diffractometers used is exceeded, and hence fringes are not visible. Especially the introduction of a distant reference signal generated by a known interface, which in the present

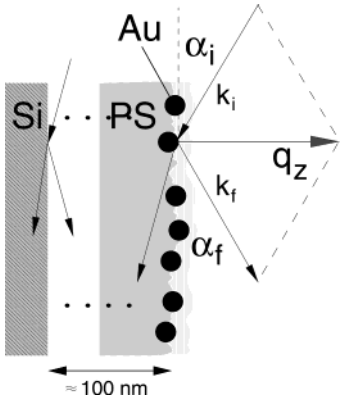

Figure 1. Sketch of a sample with a polystyrene layer (PS) on a silicon substrate, X-ray scattering geometry for reflectivity measurements. k_i and k_f denote the incident and the final wavevector, respectively. q_z refers to the vertical component of the scattering vector. The depth distribution of the clusters is consistent with the density profile at room temperature in Figure 3.

case is given by the Si/SiO_x−PS interface, significantly reduces ambiguities arising from the loss of the phase of the detected wave.[36,37] Thus, it enables an accurate determination of the unknown interfaces. A descriptive example can be found in ref 38.

A least-squares fitting analysis of the reflectivity data yields the laterally averaged electron density profile, which is proportional to the dispersion δ of the refractive index $n = 1 - \delta + i\beta$, with β being the absorption coefficient. From the change of the density profiles with increasing temperature both the embedding temperature T_e of the clusters on the surface and the glass transition temperature T_g^f of the polymer film have been extracted.

3. Results and Discussion

Figure 2 shows a representative set of X-ray reflectivity measurements for the sample with $M_w = 3.7$k and a nominal gold layer thickness $d_n = 0.7$ Å. The data are presented for selected temperatures from room temperature at $T = 303$ K (bottom) to $T = 407$ K (top), which is well above the bulk glass transition temperature $T_g^b \approx T_g^f = 351$ K. The data are normalized to the Fresnel reflectivity R_F of a silicon surface. At low q_z one observes the plateau of total external reflection. The marked values at $q_z = 0.0216$ Å^{-1} (dash−dotted line) and $q_z = 0.0318$ Å^{-1} (dashed line) correspond to the critical angles of polystyrene and silicon, respectively.

Oscillations with a short period in reciprocal space occur at wavevectors 0.03 Å$^{-1} < q_z < 0.5$ Å^{-1}. They are caused by the interference of X-rays reflected at the sample surface and the Si−PS interface. Consequently, from the period Δq_z of these oscillations the thickness of the polymer layer $d_{PS} \approx 2\pi/\Delta q_z$ can be estimated. The beating of the oscillations is caused by the gold clusters, which generate a region of increased electron density at the sample surface and hence additional length scales to the system. With increasing temperature the nodes of the beating shift toward smaller q_z values and therefore indicate an increase of distances near the sample surface due to the embedding process. The data in Figure 2 show that the shift of the first node from $q_z \approx 0.14$ Å^{-1} at 303 K to $q_z \approx 0.10$ Å^{-1} at 407 K—related with the embedding process—already starts at temperatures well below the glass transition temperature $T_g^f = 351$ K of the film.

Detailed information about the density profile of the sample can be extracted from the data by least-squares

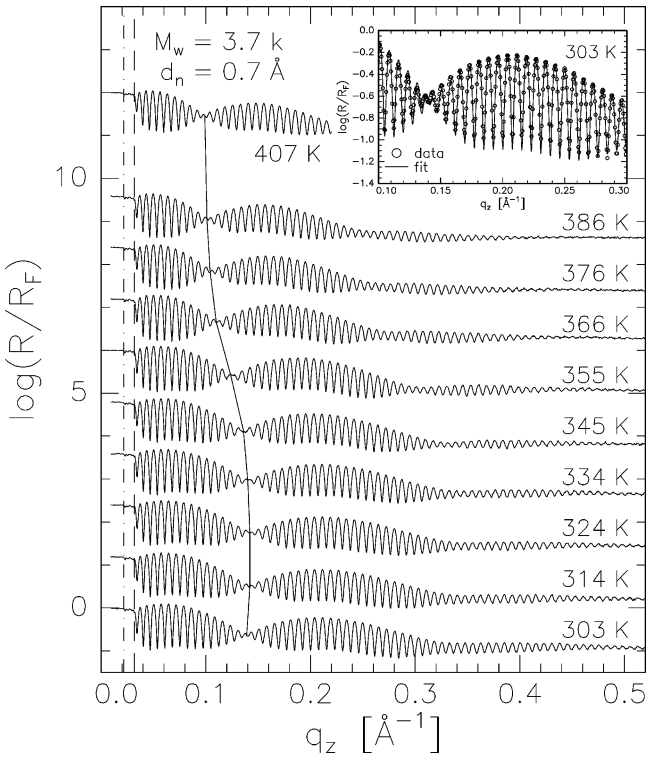

Figure 2. X-ray reflectivity data of the sample with molecular weight $M_w = 3.7$k and nominal gold layer thickness $d_n = 0.7$ Å, shifted with respect to the temperature differences. The data were taken at W1.1 at HASYLAB at an energy $E = 10.5$ keV ($\lambda = 1.181$ Å). The dash−dotted line at $q_z = 0.0216$ Å^{-1} represents the critical angle of the polystyrene and the dashed line at $q_z = 0.0318$ Å^{-1} that of silicon. The line connecting the nodes is a guide to the eye, which demonstrates the onset of changes in the near surface part of the sample. The inset shows a detailed presentation of the data measured at 303 K and the corresponding best fit.

fits on the basis of the Parratt algorithm.[39,40] Free fit parameters are the thickness of the polymer layer and the thickness, roughness, and dispersion δ related with the cluster layer at the surface of the sample. For the samples with small nominal gold layer thicknesses $d_n < 3.5$ Å (see Table 1) a tanh refractive index profile was well-suited to describe the surface profile as expected by theory[41] as well as to account for the interfaces of the gold cluster layer. Only for the data of the samples with $d_n > 3.5$ Å was a further refinement necessary to describe the interfacial profile correctly. This was done by the use of the inversion algorithm described in ref 42. The inset in Figure 2 demonstrates the high quality of the best fits gained for all measured reflectivities. They are almost indistinguishable from the data.

The near surface parts of the resulting electron density profiles for the data shown in Figure 2 and for data at additional temperatures are displayed in Figure 3. The dashed line indicates the position of the sample surface, while the solid line connects the maxima of the broad peak at 30 Å $< z <$ 50 Å, which originates from the gold clusters at the surface. As a first approximation this peak is symmetric, and hence the maximum locates the center of the cluster layer. The distance between the maximum peak position and the sample surface is denoted by $d_{vm}(T)$ and generally increases with increasing temperature. The shift of $d_{vm}(T)$ with respect to the smallest value d_0 (indicated in Figure 3 by the dash−dotted line) is denoted by $\Delta d_{vm}(T) = d_{vm}(T) - d_0$. The temperature T_e, at which the distance d_{vm} starts to

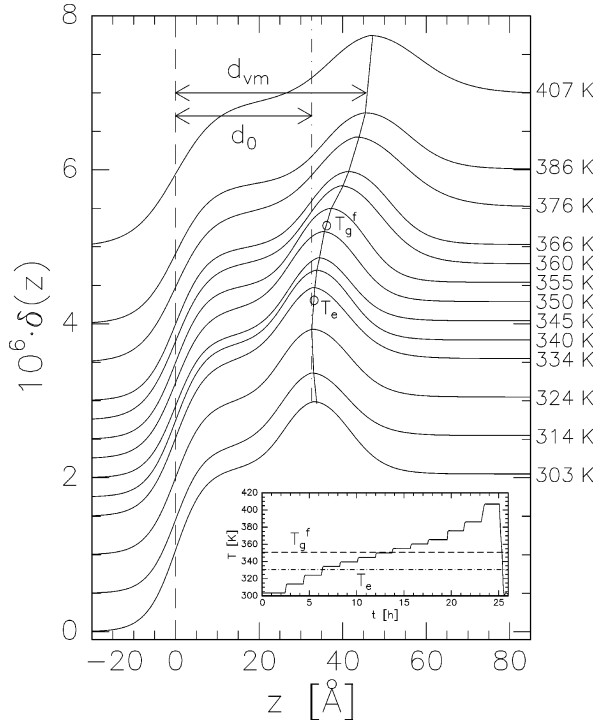

Figure 3. Electron density profiles corresponding to the data and fits shown in Figure 2 ($M_w = 3.7$k, $d_n = 0.7$ Å). The curves are shifted for clarity. The solid line connecting the maxima of the gold cluster peak serves as a guide to the eye. The distance of the maximum position to the surface at $z = 0$ (broken line) is denoted by d_{vm}. Its difference $\Delta d_{vm} = d_{vm} - d_0$ serves as a measure of the embedding process. The inset shows the temperature profile $T(\tau)$ of the sample together with the embedding temperature T_e and the glass transition temperature T_g^f of the film.

increase, is a mark for the onset of the embedding process.

Furthermore, the shape of the cluster peak changes with increasing temperature. On the given time scale it starts to broaden at a sufficiently low viscosity at temperatures of typically 10−20 K above the glass transition temperature due to the thermal motion of the gold clusters in the polymer matrix. This broadening is accompanied by an increase of the effective roughness of the interfaces as well as a decrease of the maximum of the dispersion δ of the cluster layer. These features have already been described elsewhere.[27]

It should be noted that a growth (coalescence) of the clusters with increasing temperature plays only a minor role. Recent grazing incidence small-angle scattering (GISAXS) measurements, which are also sensitive on the lateral cluster size and arrangement, have shown that this effect is small compared to the broadening of the cluster layer.[29,43]

In Figure 4, the changes of the distance $\Delta d_{vm}(T)$ as a function of temperature for a selection of samples with the lowest, an intermediate, and the highest nominal gold layer thickness d_n for the two different molecular weights are summarized (see Table 1). The left figure shows the extracted values for the temperature series of the low molecular weight polystyrene ($M_w = 3.7$k), and the right figure displays the data for the samples of high molecular weight ($M_w = 220$k). The dotted line indicates the glass transition temperature T_g^f of the film for each M_w.

The main feature of the curves is the strong increase of $\Delta d_{vm}(T)$ at temperatures above T_e (see Table 1) followed at higher temperatures $T > T_g^f$ by a region with decreasing but positive slope.

Figure 4 demonstrates that the embedding process depends strongly on the deposited amount of gold. Especially the onset of the embedding process at T_e can differ significantly from T_g^f. The intersection of a linear fit to the first two to three points of the steep part, which exceed the errors of the lowest values of Δd_{vm}, and the zero line has been used to determine the respective embedding temperature T_e. The glass transition temperatures T_g^f of the films have been obtained from the change of the coefficient of thermal expansion α_{th} of the polymer at T_g^f. This change gives rise to a different increase of the polymer layer thickness with temperature, thus marking T_g^f (see e.g. ref 40). The values for T_e and for T_g^f are listed in Table 1.

In Figure 4, an initial decrease in $\Delta d_{vm}(T)$ of about 1−2 Å at temperatures between 300 K < T < 320 K is observed. This can be explained by the desorption of some material from the sample surface, since the same effect is seen in the change of the film thickness, too.

The driving force for the embedding process is given by the contribution of the metal clusters with radius r_c to the Gibbs free energy G_c, which is lowered upon embedding. The contribution of a single, spherical cluster is given by $G_c(d) = \pi\gamma_p d^2 - 2\pi r_c(\gamma_m - \gamma_{mp})d + 2\pi r_c^2(\gamma_{mp} + \gamma_m - {}^1/_2\gamma_p)$. Here γ_m, γ_p, and γ_{mp} denote the surface or interfacial tension of the metal, the polymer, and the metal−polymer interface, respectively. d is the embedding depth from the surface to the center of the cluster.

Extensive theoretical and experimental investigations on different materials with regard to the embedding of clusters into soft matter surfaces have been carried out by Kovacs et al.[44−46] Complete embedding only is expected for $\gamma_m > \gamma_p + \gamma_{mp}$. This relation is always fulfilled for metals on polymers.

Above an embedding depth of about 10 Å the slopes of the curves in Figure 4 begin to decrease, although the dynamics at the surface should increase because of the strong decrease of the viscosity of the polymer. This indicates that the main driving force due to the reduction in surface energy has ceased because the clusters are completely embedded. The further increase of $\Delta d_{vm}(T)$ in this temperature regime is caused, as mentioned before, by diffusion of the clusters in the polymer, which leads to an anisotropic broadening of the cluster peak in the electron density profile[27] and therefore to a net displacement of the center of the cluster layer.

The graphs in Figure 5 show the determined embedding temperatures T_e as a function of the nominal gold layer thickness d_n for the two different molecular weights of $M_w = 3.7$k and $M_w = 220$k. The mean glass transition temperatures T_g^f of the films including their errors are also displayed. A significant drop in the embedding temperature T_e can be seen when d_n approaches zero. This strongly suggests that there is a significant influence of the gold on the mobility of the polymer chains.

To explain this dependence, at least two aspects have to be discussed, i.e., (i) the variation of the cluster radius r_c with varying nominal gold layer thickness d_n and (ii) the interaction between the clusters and the polymer. The latter is related with the number density of clusters on the surface n_c under consideration of the cluster size,

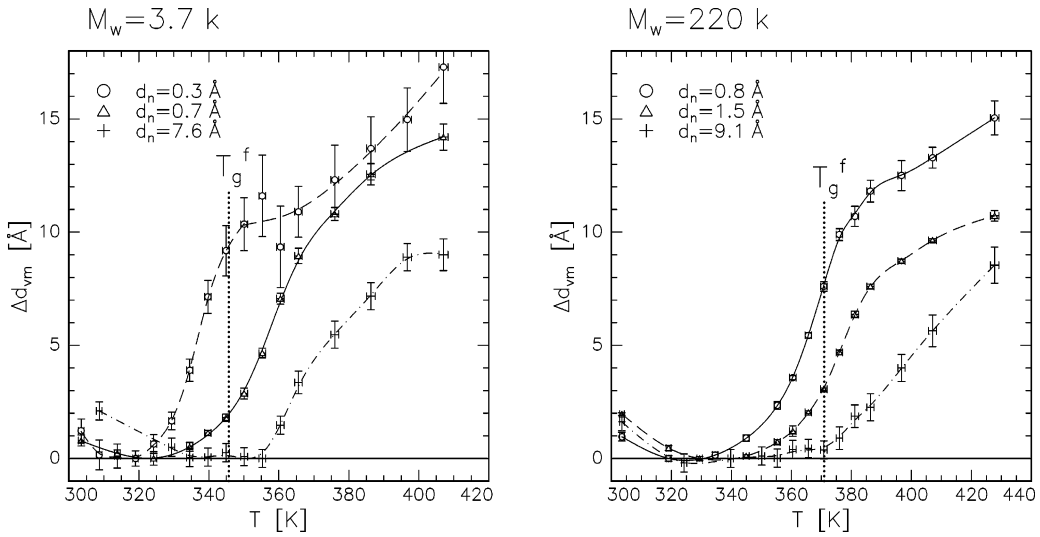

Figure 4. Change in the distance Δd_{vm} between the sample surface and the maximum of the cluster layer. A series of three representative nominal gold layer thicknesses are shown, on the left for polystyrene with $M_w = 3.7$k and on the right with $M_w =$ 220k. The dotted line indicates the location of the glass transition temperature T_g^f of the polymer layer.

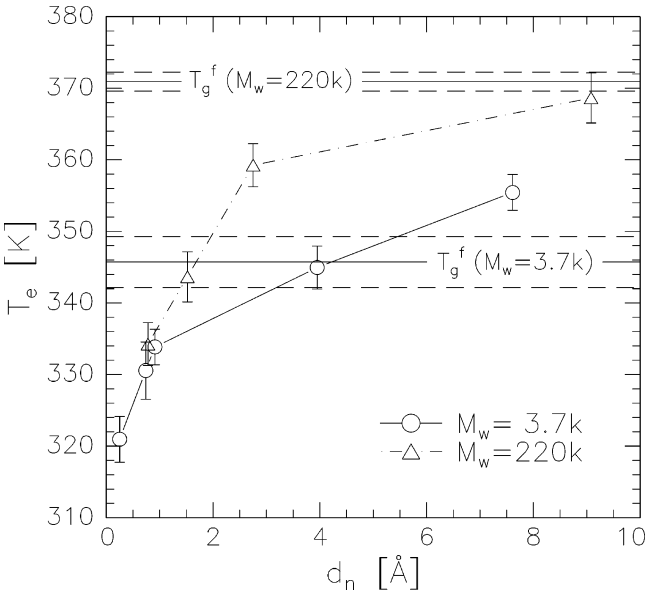

Figure 5. Embedding temperatures T_e as a function of the nominal gold layer thickness d_n for two different molecular weights ($M_w = 3.7$k and $M_w = 220$k). The mean glass transition temperature T_g^f from all measured samples and its error are indicated.

which is given by the fraction f of the surface covered by clusters. This fraction is proportional to the contact area of equally embedded clusters and can be regarded as a measure of these interactions.

The differences in cluster size play a minor role to explain the decrease of T_e for small d_n. Only in the case that the differences in cluster size exceed the persistence length of polystyrene[47,48] $l_p \approx 15$ Å, which gives a measure of the minimum distance for the polymer to behave as a freely rotating chain, significant size effects should occur. In this work the differences in cluster diameter between the smallest clusters of $r_c = 9$ Å and the largest ones with $r_c = 18$ Å are rather small, i.e., of the order of l_p. Moreover, even differences in the cluster radius of only 2 Å have caused significantly different embedding temperatures T_e (see Table 1).

Therefore, the interaction between the gold and the polystyrene plays the major role concerning the increase of T_e with increasing d_n. An estimate of the interaction between the clusters and the polymers on the basis of van der Waals forces—which provide a long-range interaction—has already been given in ref 27. The material-dependent Hamaker constants A serve as a measure of the strength due to dispersion forces. The relevant values are for the interaction between the polystyrene molecules, $A_{PS,PS} = 6.5 \times 10^{-20}$ J, for the interaction between gold and polystyrene, $A_{Au,PS} = 17.1 \times 10^{-20}$ J, and for the interaction between the gold clusters via the polymer, $A_{Au,PS,Au} = 30.8 \times 10^{-20}$ J.[49,50] These Hamaker constants strongly suggest that the interaction between the gold and the polymer is about 2.6 times larger than that between adjacent polymer chains. Thus, the mobility of the polymer chains in the vicinity of the clusters is reduced, which leads to an increase of T_e with increasing total surface area of the clusters, given by an increase of d_n.

Investigations on the diffusion of single metal atoms in polymers suggest that there are even stronger interactions than the long-range van der Waals forces considered so far. It has been found that the diffusion coefficient of noble gases in amorphous polymers is several orders of magnitude larger than that of noble metals.[31] This has been explained by a strong local immobilization of the polymer chains near the metal atoms due to a short-range interaction between the metal and the polymer.

Using infrared reflection−absorption spectroscopy (IRAS) and near-edge X-ray absorption fine structure spectroscopy (NEXAFS), Strunskus et al.[51] revealed that on a gold−polyimide system there are no "chemical" interactions between the metal clusters and the polymer chains. They state that only a "purely physical interaction mechanism" has to be considered for noble metals on polyimide surfaces.

Nevertheless, Cole et al.[52] pointed out that even much weaker interactions than those accessible by the methods Strunskus et al. applied affect the mobility of the polymer segments. For the system Au−poly(*tert*-butyl acrylate) they found a decrease of the mobility of gold particles by 2−3 orders of magnitude compared to what is expected by the Stokes−Einstein relation. They attributed their results to "bridging interactions between particles" governed by the polymer molecules in

contact with clusters. They also state that those polymers not in contact with the gold clusters would by able to "move relatively freely through the system".

The origin of the additional short-range interaction is related with the overlap between electron clouds of the gold and the polymer, giving rise to an interaction energy exceeding the one due to van der Waals interactions. The mean number of contact sites per cluster, which is proportional to the total cluster surface adjacent to the polymer, can be regarded as a measure of the strength of this interaction.

For the present study these results indicate that due to the additional short-range interactions around each gold cluster, a spherical region exists with strongly reduced mobility of the polymer chains. The total radius of this sphere is the sum of the cluster radius r_c and the persistence length l_p. Consequently, if the clusters were too close to each other, the embedding is expected to happen at embedding temperatures even above T_g^f. Indeed, this has been observed in the present study for the sample with $M_w = 3.7$k and $d_n = 7.6$ Å. If about half of the surface is covered, which corresponds to $d_n \approx 17$ Å, no embedding is observed at all (see Table 1).

Because of the polymer−metal interactions, which cannot be neglected, the glass transition temperature of the unperturbed polystyrene surface T_g^s can be regarded as the embedding temperature in the limit of a vanishing amount of gold, i.e., $T_g^s = \lim_{d_n \to 0} T_e$. A linear extrapolation of the determined T_e in Figure 5 for $d_n \to 0$ using the first three data points yields $T_g^s \approx (316 \pm 5)$ K for $M_w = 3.7$k and $T_g^s \approx (325 \pm 5)$ K for $M_w = 220$k. The measured upper limits given by the lowest coverages in this work are $T_e = 321$ K for $M_w = 3.7$k and $T_e = 334$ K for $M_w = 220$k.

An extension of data points in Figure 5 to lower coverages is desirable but prevented by two constraints: (i) The smallest possible "clusters", single atoms, are capable of diffusing into the bulk polymer well below the glass transition temperature.[31] This is a consequence of the free volume of the polymer, which is quite large compared to that of crystalline materials. Therefore, single atoms cannot be used as "markers" for the surface glass transition temperature.

(ii) The low scattering contrast of a diluted cluster layer significantly aggravates the analysis of the X-ray reflectivity data. Moreover, for low coverages the roughness caused by thermally activated capillary waves is of the order of the radius of the clusters. Since the height distribution of the clusters on the polymer surface is given by this roughness, the height of the cluster peak in the electron density profile is small compared to the width of the peak. This leads to a damping of the characteristic beating related to the cluster layer.

4. Conclusions

In situ X-ray reflectivity measurements of polystyrene films decorated with gold nanoclusters have been performed. With increasing temperature the relaxation of the samples at the glass transition temperature is accompanied by (i) an embedding process at the sample surface and (ii) a change in the coefficient of thermal expansion α_{th} of the polymer film. While the embedding process of the clusters can be regarded as a probe of the glass transition at the surface, the change in α_{th} is a measure of the glass transition temperature of the polymer layer, corresponding to the bulk value T_g^b. For low nominal gold layer thicknesses $d_n < 3.5$ Å, the embedding of the clusters always takes place at temperatures below T_g^b, which is due to the increased mobility of the polymer segments at the surface compared to those in the bulk. It has been shown that the embedding process strongly depends on the amount of gold deposited on the sample surface. This indicates a strong short-range polymer−metal interaction. This interaction very likely exceeds the long-range van der Waals forces and hence notably reduces the mobility of the polymer chains in the vicinity of the clusters. Thus, the embedding temperatures T_e provide upper limits of the glass transition temperature T_g^s at the surface of a pure polymer layer without clusters. However, if the nominal gold layer thickness d_n approaches zero, the embedding of small particles indeed can be regarded as a measure of the glass transition temperature of the polymer in a very narrow surface region.

Acknowledgment. We thank Oliver Seeck, beamline scientist at W1.1 at HASYLAB, for his skillful help during the beamtimes at W1.1 and for the latest version of "reflek". We gratefully acknowledge Jörn Erichsen and Prof. F. Faupel for the preparation of the polymer layers and helpful discussions. We also thank Bridget Murphy, Claas Behrend, and Klaas Kölln for their great help during many beamtimes and Prof. Pehlke for his valuable hints concerning the polymer−metal interactions. This work was supported by the "Deutsche Forschungsgemeinschaft" (DFG project Pr325/12-1).

References and Notes

(1) Mittal, K. L., Ed. *Metallized Plastics: Fundamentals and Applications*; Marcel Dekker: New York, 1998.
(2) Wong, C. P., Ed. *Polymers for Electronic and Photonic Applications*; Academic Press: Boston, 1993.
(3) Keddie, J. L.; Jones, R. A. L.; Cory, R. A. *Europhys. Lett.* **1994**, *27*, 59.
(4) Wallace, W. E.; van Zanten, J. H.; Wu, W. L. *Phys. Rev. E* **1995**, *52*, R3329.
(5) van Zanten, J. H.; Wallace, W. E.; Wu, W. L. *Phys. Rev. E* **1996**, *53*, R2053.
(6) Forrest, J. A.; Dalnoki-Veress, K.; Stevens, J. R.; Dutcher, J. R. *Phys. Rev. Lett.* **1996**, *77*, 2002; *Phys. Rev. Lett.* **1996**, *77*, 4108.
(7) Forrest, J. A.; Dalnoki-Veress, K.; Dutcher, J. R. *Phys. Rev. E* **1997**, *56*, 5705.
(8) Grohens, Y.; Brogly, M.; Labbe, C.; David, M. O.; Schultz, J. *Langmuir* **1998**, *14*, 2929.
(9) Forrest, J. A.; Jones, R. A. L. In *Polymer Surfaces, Interfaces and Thin Films*; Karim, A., Kumar, S., Eds.; World Scientific: Singapore, 2000.
(10) Chow, T. S. *J. Phys.: Condens. Matter* **2002**, *14*, L333.
(11) Varnik, F.; Baschnagel, J.; Binder, K. *Phys. Rev. E* **2002**, *65*, 021507.
(12) Kajiyama, T.; Tanaka, K.; Takahara, A. *Macromolecules* **1997**, *30*, 280.
(13) Kajiyama, T.; Tanaka, K.; Takahara, A. *Polymer* **1998**, *39*, 4665.
(14) Satomi, N.; Takahara, A.; Kajiyama, T. *Macromolecules* **1999**, *32*, 4474.
(15) Hammerschmidt, J. A.; Gladfelter, W. L.; Haugstad, G. *Macromolecules* **1999**, *32*, 3360.
(16) Tsui, O. K. C.; Wang, X. P.; Ho, J. Y. L.; Ng, T. K.; Xiao, X. *Macromolecules* **2000**, *33*, 4198.
(17) Liu, Y.; Russell, T. P.; Samant, M. G.; Stöhr, J.; Brown, H. R.; Cossy-Favre, A.; Diaz, J. *Macromolecules* **1997**, *30*, 7768.
(18) Ge, S.; Pu, Y.; Zhang, W.; Rafailovich, M.; Sokolov, J.; Buenviaje, C.; Buckmaster, R.; Overney, R. M. *Phys. Rev. Lett.* **2000**, *85*, 2340.
(19) Forrest, J. A. *Eur. Phys. J. E* **2002**, *8*, 261.
(20) Kerle, T.; Lin, Z.; Kim, H.-C.; Russell, T. P. *Macromolecules* **2001**, *34*, 3484.
(21) Hamdorf, M.; Johannsmann, D. *J. Chem. Phys.* **2000**, *112*, 4262; *J. Chem. Phys.* **2001**, *114*, 9685.

(22) Petersen, K.; Johannsmann, D. *J. Non-Cryst. Solids* **2002**, *307*−*310*, 532.
(23) Zaporojtchenko, V.; Strunskus, T.; Erichsen, J.; Faupel, F. *Macromolecules* **2001**, *34*, 1125.
(24) Erichsen, J.; Günther-Schade, K.; Dolgner, K.; Strunskus, T.; Zaporojtchenko, V.; Faupel, F. *Mater. Res. Soc. Symp. Proc.* **2002**, *710*.
(25) Rudoy, V. M.; Dement'eva, O. V.; Yaminskii, I. V.; Sukhov, V. M.; Kartseva, M. E.; Ogarev, V. A. *Colloid J.* **2002**, *64*, 746.
(26) Teichroeb, J. H.; Forrest, J. A. *Phys. Rev. Lett.* **2003**, *91*, 016104.
(27) Weber, R.; Zimmermann, K.-M.; Tolan, M.; Stettner, J.; Press, W.; Seeck, O. H.; Erichsen, J.; Zaporojtchenko, V.; Strunskus, T.; Faupel, F. *Phys. Rev. E* **2001**, *64*, 061508.
(28) Erichsen, J., unpublished work, 2002.
(29) Weber, R. Ph.D. Thesis, University of Kiel, 2002.
(30) Venables, J. A. *Surf. Sci.* **1994**, *299/300*, 798.
(31) Faupel, F.; Willecke, R.; Thran, A. *Mater. Sci. Eng.* **1998**, *R22*, 1.
(32) von Bechtolsheim, C.; Zaporojtchenko, V.; Faupel, F. *Appl. Surf. Sci.* **1999**, *151*, 119.
(33) Zaporojtchenko, V.; Strunskus, T.; Behnke, K.; von Bechtolsheim, C.; Kiene, M.; Faupel, F. *J. Adhes. Sci. Technol.* **2000**, *14*, 467.
(34) Jacobs, K.; Herminghaus, S.; Mecke, K. R. *Langmuir* **1998**, *14*, 965.
(35) Kiessig, H. *Ann. Phys.* **1931**, *10*, 769.
(36) Sivia, D. S.; Hamilton, W. A.; Smith, G. S.; Rieker, T. P.; Pynn, R. *J. Appl. Phys.* **1991**, *70*, 732.
(37) Majkrzak, C. F.; Berk, N. F. *Physica B* **1996**, *221*, 520.
(38) Stettner, J.; Schwalowsky, L.; Seeck, O. H.; Tolan, M.; Press, W.; Schwarz, C.; von Känel, H. *Phys. Rev. B* **1996**, *53*, 1398.
(39) Parratt, L. G. *Phys. Rev.* **1954**, *95*, 359.
(40) Tolan, M. *X-Ray Scattering from Soft-Matter Thin Films*; Springer Tracts in Modern Physics; Springer-Verlag: Berlin, 1999; Vol. 148.
(41) Helfand, E.; Tagami, Y. *J. Chem. Phys.* **1972**, *56*, 3592.
(42) Zimmermann, K.-M.; Tolan, M.; Weber, R.; Stettner, J.; Doerr, A. K.; Press, W. *Phys. Rev. B* **2000**, *62*, 10377.
(43) Chamard, V., unpublished work.
(44) Kovacs, G. J.; Vincett, P. S. *J. Colloid Interface Sci.* **1982**, *90*, 335.
(45) Kovacs, G. J.; Vincett, P. S.; Tremblay, C.; Pundsack, A. L. *Thin Solid Films* **1983**, *101*, 21.
(46) Kovacs, G. J.; Vincett, P. S. *Thin Solid Films* **1984**, *111*, 65.
(47) Flory, P. J. *Statistical Mechanics of Chain Molecules*; John Wiley & Sons: New York, 1969.
(48) Strobl, G. R. *The Physics of Polymers*; Springer-Verlag: Berlin, 1997.
(49) Krupp, H.; Schnabel, W.; Walter, G. *J. Colloid Interface Sci.* **1972**, *39*, 421.
(50) Parsegian, V. A.; Weiss, G. H. *J. Colloid Interface Sci.* **1981**, *81*, 285.
(51) Strunskus, T.; Grunze, M.; Kochendoerfer, G.; Wöll, Ch. *Langmuir* **1996**, *12*, 2712.
(52) Cole, D. H.; Shull, K. R.; Rehn, L. E.; Baldo, P. *Phys. Rev. Lett.* **1997**, *78*, 5006.

MA034880O